

Crosstalk analysis for single-qubit and two-qubit gates in spin qubit arrays

Irina Heinz^{✉*} and Guido Burkard^{✉†}

Department of Physics, University of Konstanz, D-78457 Konstanz, Germany



(Received 21 May 2021; revised 30 June 2021; accepted 9 July 2021; published 20 July 2021)

Scaling up spin qubit systems requires high-fidelity single-qubit and two-qubit gates. Gate fidelities exceeding 98% were already demonstrated in silicon-based single and double quantum dots, whereas for the realization of larger qubit arrays, crosstalk effects on neighboring qubits must be taken into account. We analyze qubit fidelities impacted by crosstalk when performing single-qubit and two-qubit operations on neighbor qubits with a simple Heisenberg model. Furthermore, we propose conditions for driving fields to robustly synchronize Rabi oscillations and avoid crosstalk effects. In our analysis, we also consider crosstalk with two neighbors and show that double synchronization leads to a restricted choice for the driving field strength, exchange interaction, and thus gate time. Considering realistic experimental conditions, we propose a set of parameter values to perform a nearly crosstalk-free CNOT gate and so open up the pathway to scalable quantum computing devices.

DOI: [10.1103/PhysRevB.104.045420](https://doi.org/10.1103/PhysRevB.104.045420)

I. INTRODUCTION

Spin qubits [1] in silicon quantum dots [2] are a promising candidate to realize large scale quantum computers [3]. Due to the dilute nuclear spin environment and weak spin-orbit coupling, silicon enables long coherence times and high-fidelity spin manipulation [4]. Single-qubit gates can be implemented via electric dipole spin resonance (EDSR) by modulating electrostatic gate voltages causing motion of the dot electrons. Two-qubit gates additionally make use of exchange interactions between neighboring electron spins [5–9] operating at a symmetric operation point (“sweet spot”) to suppress charge noise to first order [10–12]. Dephasing effects can be reduced through a large energy splitting due to a strong magnetic field gradient [13] realized by a micromagnet [14,15].

High-fidelity CNOT gate implementations have already been proposed and demonstrated in a Si/SiGe heterostructure double quantum dot architecture [8,16]. Nevertheless, scalable spin qubit platforms [17,18] suffer from unwanted interactions of qubits with the environment and fluctuations of interacting fields yielding crosstalk, dephasing, and charge noise, which represent challenges for experimental realization. Hence, a better understanding of the underlying effects is crucial for error prevention and thus high-fidelity performance of gates within qubit arrays. In this paper, we focus on crosstalk effects of single-qubit and two-qubit gates on neighboring qubits induced, e.g., by capacitive coupling between gates, which can decrease the fidelity by several percent [19]. Here, we concentrate on crosstalk and disregard pure gate errors affecting operating qubits, which have been studied extensively [6,10,19].

This paper is organized as follows. For our description, we consider a Heisenberg spin model in Sec. II. On this

basis, we quantify crosstalk in terms of neighboring qubit fidelity in Sec. III and address the responsible values to reduce crosstalk errors with simple synchronizations in Sec. IV. For single-qubit rotations around the y axis, we also consider second-neighbor and next-nearest-neighbor coupling leading to off-resonant Rabi oscillations, which also occur in systems driven with global striplines [20,21], and give a possible cancellation condition for unwanted rotations. Similarly, we suggest a double synchronization and a thoughtful choice of values for EDSR driving and exchange interaction strengths to implement mostly crosstalk-free CNOT gates in spin qubit arrays in Sec. IV B. In Sec. V, we determine the crosstalk of simultaneously driven single-qubit operations which are applied in quantum algorithms and give conditions to maximize the overall fidelity. Finally, to evaluate the robustness of synchronizing Rabi frequencies, we analyze the impact of charge noise on the fidelity in Sec. VI.

II. THEORETICAL MODEL

For our analysis, we consider a gate defined linear quantum dot array operated in the $(1, 1, \dots)$ charge regime, where the exchange interaction between two spins can be tuned by middle barrier gates, such as in Refs. [16] and [8] (Fig. 1). Neglecting excited valley states and spin-orbit coupling, the system can be described theoretically by the Heisenberg Hamiltonian,

$$H = \sum_{\langle i,j \rangle} J_{ij}(t) \left(\mathbf{S}_i \cdot \mathbf{S}_j - \frac{1}{4} \right) + \sum_i \mathbf{S}_i \cdot \mathbf{B}_i, \quad (1)$$

where J_{ij} is the tunable exchange interaction between nearest-neighbor spins \mathbf{S}_i and \mathbf{S}_j , denoted by $\langle i, j \rangle$, required for two-qubit operations, and $\mathbf{B}_i = (0, B_{y,i}(t), B_{z,i})$ is the external magnetic field at the position of spin \mathbf{S}_i . Magnetic fields are represented in energy units throughout this paper, i.e., $\mathbf{B}_{\text{physical}} = \mathbf{B}/g\mu_B$, and we furthermore set $\hbar = 1$. The total

*irina.heinz@uni-konstanz.de

†guido.burkard@uni-konstanz.de

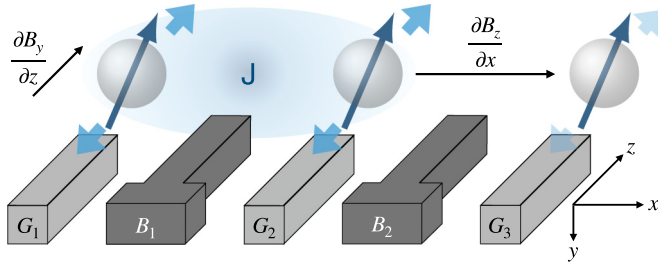


FIG. 1. Schematic setup for a gate defined linear array of three quantum dots inside a large homogeneous magnetic field (not shown) and a magnetic gradient field as, e.g., induced by a micromagnet. Each dot is occupied with an electron representing a qubit with distinguishable spin resonance frequencies enabled by the gradient $\partial B_z/\partial x$. Modulations of gate voltages G_1 and G_2 shift the respective electrons in the z direction along the gradient $\partial B_y/\partial z$ such that an effective oscillating magnetic field is generated. This also leads to crosstalk on a neighboring qubit at gate G_3 . Exchange interaction J between two spins is controlled by electrostatic voltages at the middle barrier gates B_1 and B_2 and is required for two-qubit operations.

magnetic field consists of a large homogeneous field and a field gradient in the z direction along the x axis (see Fig. 1), e.g., caused by a micromagnet, $B_{z,i} = B_z + b_{z,i}$, allowing one to individually address single spins, and a small field gradient, such as a time-dependent EDSR driving field in the y direction, $B_{y,i}(t) = B_{y0,i} + B_{y1,i} \cos(\omega t + \theta)$. The latter in general can describe ESR or EDSR, where the effective magnetic driving strength for EDSR is proportional to the electric field depending on the device architecture, natural or artificial spin-orbit coupling mechanism, and applied gate voltage [22,23]. In the rotating frame $\tilde{H}(t) = R^\dagger H R + i\dot{R}^\dagger R$, with $R = \exp(-i\omega t \sum_i S_i)$, we make the rotating wave approximation (RWA), which results in resonant and off-resonant Rabi terms. To evaluate the crosstalk of single-qubit and two-qubit gates on the neighboring qubit, we calculate the fidelity [24],

$$F = \frac{d + |\text{Tr}[U_{\text{ideal}}^\dagger U_{\text{actual}}]|^2}{d(d+1)}, \quad (2)$$

where d is the dimension of the Hilbert space, U_{ideal} is the desired qubit operation, which in the case of crosstalk would be $\mathbb{1}$ for the neighboring qubits, and U_{actual} is the actual operation containing unwanted off-resonant Rabi oscillations with a detuned Rabi frequency,

$$\tilde{\Omega} = \sqrt{\Omega^2 + \delta\omega_z^2}. \quad (3)$$

Here, Ω denotes the resonant Rabi frequency and $\delta\omega_z$ is the detuning between driving and resonance frequencies.

III. CROSSTALK ANALYSIS

In the following, we always consider a gate performed on qubit 1 (1 and 2) for single-qubit (two-qubit) operations and their corresponding crosstalk on the nearest-neighbor qubit 2 (3) in the form of an unwanted magnetic driving field on the neighboring qubit, which for EDSR can be capacitively induced [25,26] by the actual driving field $B_{y1,1}$ ($B_{y1,2}$) applied on the corresponding gate [27].

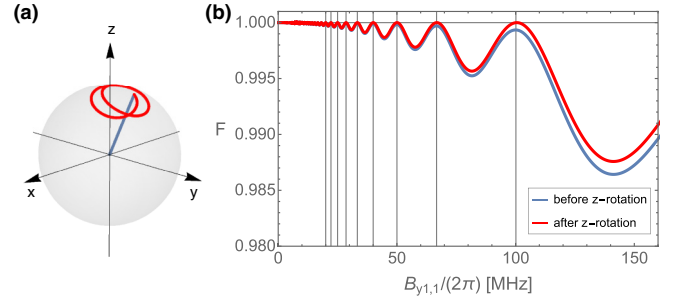


FIG. 2. Fidelity of neighbor qubit 2 remaining in its state while driving a Y gate on qubit 1 at resonance frequency $B_{z,1} = (2\pi)18.493$ GHz assuming $\alpha = 0.4$. (a) Off-resonant Rabi oscillations of qubit 2 in a Bloch sphere representation. (b) Fidelity depending on driving strength $B_{y1,1}$ (blue) shows maxima if the synchronization condition (7) is fulfilled. Fidelity after the subsequent z rotation (red) leads to no effective crosstalk at synchronization conditions. Here, $\Delta B_z = (2\pi)0.2$ MHz, $B_{y1,2} = \alpha B_{y1,1}$, and $\alpha = 0.4$.

A. Single-qubit gate: Y gate

For a complete set of single-qubit gates, rotations around two axes are required. Since z rotations can simply be implemented in software by incorporating the rotation angle in the phase of the microwave pulse [8], we focus on the performance of y rotations, which are realized by driving the operating qubit 1 at its resonance frequency, $\omega_{z,1} = B_{z,1}$ (a similar analysis is possible for X and other single-qubit gates). The capacitive coupling between the gate electrodes and the single electrons representing qubits can lead to a small effective magnetic field at neighboring qubit 2, which results in an off-resonant Rabi oscillation with detuned Rabi frequency given by Eq. (3), where the resonant Rabi frequency is $\Omega_2 = B_{y1,2}/2$ and the detuning amounts to $\delta\omega_{z,2} = B_{z,2} - B_{z,1}$. For numerical examples, we assume a resonance frequency for $B_{z,1}$ of $(2\pi)18.493$ GHz as in Ref. [8], and vary the nearest-neighbor qubit crosstalk field $B_{y1,2}$ as well as the z -field gradient $\Delta B_z = B_{z,2} - B_{z,1}$, and investigate the fidelity of the idle qubit 2. We find that with increasing $B_{y1,2}$, the driving strength becomes larger and the fidelity oscillates and decreases, as shown in Fig. 2(b). On the other hand, the increasing field gradient in the z direction causes the resonance frequencies of the single qubits to further diverge and leads to further off-resonant Rabi oscillations such that the fidelity increases.

To verify the accuracy of the RWA used for the fidelity calculations, we take into account higher-order corrections within the Floquet-Magnus expansion (FME) for periodically driven systems [28–31], and compare RWA with FME corrected fidelities in Appendix A. Although the main contribution to the corrections comes from the nonvanishing part of $B_{y0,2}$, which is neglected in the RWA, the fidelity only slightly changes even for very large values of $B_{y0,2}$ compared to the driving field $B_{y1,2}$. Since for micromagnet-induced inhomogeneous fields the gradient field in the y direction is typically considerably smaller than $B_{y1,2}$ [14,32], we find that indeed the RWA is a good approximation for the relevant regime of operation.

B. Two-qubit gate: CNOT gate

Two-qubit gates between neighboring qubits (in our case, qubits 1 and 2) can be performed by switching on their exchange interaction as depicted in Fig. 1. A CNOT gate can be implemented by adiabatically switching on $J_{12} = J$ to shift energy levels such that distinct transition frequencies allow individual addressing of the $|10\rangle \leftrightarrow |11\rangle$ transition. Combined with a driving field matching the appropriate transition frequency, this results in a CNOT gate (Ω_{CNOT}) with an off-resonant Rabi oscillation (Ω_{off}) that can be canceled out by a simple synchronization of Rabi frequencies [16],

$$\Omega_{\text{CNOT}} = \frac{2m+1}{2n} \tilde{\Omega}_{\text{off}}, \quad m, n \in \mathbb{Z}, \quad (4)$$

which we will refer to as the CNOT synchronization in the remainder of this paper. Assuming that the middle barrier gate determining J has no effective capacitive coupling due to application of improved virtual gates [33–35] and therefore does not affect the neighboring qubits, the remaining effect contributing to crosstalk is a resulting driving field at the neighboring qubit 3. This turns out to be the same effect as for single-qubit gates with different driving frequency, $\omega_{\text{CNOT}} = (B_{z,1} + B_{z,2} + J - \sqrt{(B_{z,2} - B_{z,1})^2 + J^2})/2$, and thus different off-resonant Rabi-oscillations due to the detuning, $\delta\omega_z = B_{z,3} - \omega_{\text{CNOT}}$. Calculating the fidelity depending on the resulting driving field $B_{y,1,3}$ at neighboring qubit 3, the magnetic field gradient ΔB_z indeed shows a similar behavior to the case of single-qubit gate crosstalk (Fig. 2). Since we operate in the $J \ll \Delta B_z$ regime, varying the exchange interaction J only leads to small-amplitude oscillations of the fidelity.

IV. SCHEMES TO AVOID CROSSTALK

Now that crosstalk of single-qubit and two-qubit gates can be quantified, we suggest schemes minimizing these effects to reduce errors when scaling up qubit architectures beyond existing dynamical decoupling protocols [36,37].

Off-resonant Rabi oscillations caused by driving a neighboring qubit to perform Y or CNOT gates are combined rotations around the y and z axes, as shown in the Bloch sphere representation in Fig. 2(a). Since z rotations can be canceled easily via software, we can find a subsequent rotation to minimize crosstalk and thus to maximize the fidelity. For the Y gate, fidelities are compared to those after following z rotations as in Fig. 2(b), and indeed, this results in a better performance. Similarly, fidelity improving z rotations can also be found for two-qubit gates such as the CNOT.

In analogy to virtual gates for dc voltages defined by capacitance matrices [38,39], one could think of a similar approach for an ac drive, where neighboring gates would have opposite driving amplitudes but the same frequency. This would cancel out driving amplitudes on neighboring qubits and so would avoid crosstalk effects. However, the ac virtual gate strategy requires high-precision control in experiments and could lead to further noise through fluctuating magnetic driving amplitudes.

A different approach, which can also be relevant for systems driving qubits with a global stripline as in [20] and [21], is the synchronization of Rabi frequencies, similar to the one in Eq. (4) of Ref. [16]. We require that during the driving time

τ to perform spin rotations, the neighboring spin shall do only full 2π rotations,

$$\tilde{\Omega}\tau = 2\pi k, \quad k \in \mathbb{Z}, \quad (5)$$

with the detuned Rabi frequency $\tilde{\Omega}$. Further defining

$$\alpha = \frac{B_{\text{NN}}}{B_{\text{drive}}}, \quad (6)$$

as the ratio between the induced driving amplitude B_{NN} at the nearest-neighbor qubit 2 (3) and the actual driving strength B_{drive} on qubit 1 (1 and 2), a condition for B_{drive} can be expressed in terms of α .

A. Synchronization for the Y gate

In the case of the Y gate where $B_{\text{drive}} = B_{y,1,1}$ and $B_{\text{NN}} = B_{y,1,2}$ we obtain $\tilde{\Omega} = \tilde{\Omega}_2 = \sqrt{(B_{y,1,2}/2)^2 + (\Delta B_z)^2}$ for the off-resonant Rabi frequency of qubit 2. Since the time to perform a π rotation on qubit 1 is $\tau_Y = \pi(2m+1)/\Omega_1$ where $m \in \mathbb{Z}$ with resonant Rabi frequency $\Omega_1 = B_{y,1,1}/2$, we obtain

$$B_{y,1,1} = \frac{2\Delta B_z}{\sqrt{\frac{4k^2}{(2m+1)^2} - \alpha^2}}, \quad (7)$$

as the synchronization condition for integers k and m . For $\alpha = 0$, the remaining oscillation is around the z axis and can be neglected; for $0 < \alpha < 1$, the fidelity reaches a maximum when condition (7) is fulfilled. In Fig. 2(b), for $\alpha = 0.4$, the fidelity is plotted in dependence on $B_{y,1,1}$. Repeated fidelity maxima occur when the synchronization condition (7) is satisfied. The red line of Fig. 2(b) contains a subsequent z rotation, which at the maxima in fact leads to fidelities of 1, and thus to the complete absence of crosstalk effects.

So far, we only considered one neighboring qubit next to the operation qubit. However, in quantum dot arrays, each qubit has multiple neighbors, e.g., two neighbors in a linear array. For the Y gate, we now consider two neighboring qubits 2 and 3, with crosstalk amplitudes $B_{y,1,2} = \alpha B_{y,1,1}$ and $B_{y,1,3} = \tilde{\alpha} B_{y,1,1}$, respectively. Assuming the same gradient in the z direction, for each neighbor $|B_{z,3} - B_{z,1}| = |B_{z,2} - B_{z,1}| = \Delta B_z$, condition (7) must be fulfilled for each neighbor with α or $\tilde{\alpha}$ and integers k and l , where l replaces k in condition (7) for qubit 3. Since both conditions need to be simultaneously satisfied, this leads to restricted solutions for $\tilde{\alpha}$ depending on α , k , l , and m . To showcase some configurations for which such a double synchronization is possible, we choose $\alpha = 0.4$ and $k = 1$ and represent solutions for $\tilde{\alpha}$ depending on l for several values m in Fig. 3 by dots. Besides trivial solutions, we find only discrete values for $0 < \tilde{\alpha} < 1$. Additionally, varying k allows for further discrete values for $\tilde{\alpha}$. As a consequence, this means that if hardware can be implemented precisely enough to determine the capacitive couplings α and $\tilde{\alpha}$, such that they match both synchronization conditions, crosstalk on both neighbors can be completely prevented. Alternatively, one could adapt this condition to synchronize next-nearest-neighbor qubits within a quantum dot array by modifying α and $\tilde{\alpha}$ and the gradient field, respectively. Note that higher m values have a direct impact on the gate time due to the $\tau_Y \propto 2m+1$ scaling of a π pulse.

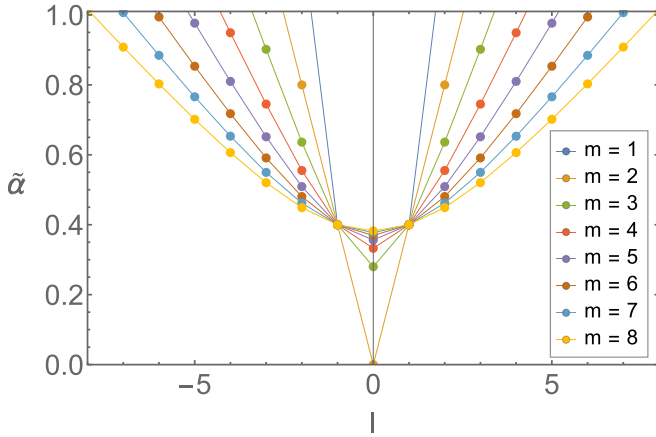


FIG. 3. Solutions $\tilde{\alpha}$ for combinations of l and m matching the synchronization condition (7) of a Y gate for two nearest-neighbor qubits with $k = 1$ and $\alpha = 0.4$.

In general, each qubit needs to be individually characterized and differs from others due to fabrication. Therefore, the above assumption for equal z -gradient fields must be adapted. Typically, α and $\tilde{\alpha}$ cannot be chosen but are predetermined by the system and can be obtained, e.g., by measuring frequencies of off-resonant Rabi oscillations. Although a general exact double synchronization for arbitrary α and $\tilde{\alpha}$ is not possible, crosstalk reduction can still be realized by choosing a configuration of k , l , and m , such that the synchronization condition is nearly fulfilled.

B. Synchronization for the CNOT gate

To perform a high-fidelity CNOT gate on qubits 1 and 2, the synchronization of Rabi frequencies in Eq. (4) is advantageous. Similar to previous double synchronization, we would like to find solutions which additionally satisfy the crosstalk cancellation condition (5). As shown in Ref. [16], for equal driving fields $B_{y1,1} = B_{y1,2}$, the CNOT synchronization yields

$$B_{y1,1} = \pm \frac{2J}{\sqrt{\frac{4n^2}{(2m+1)^2} \left(1 + \frac{J}{2\Delta B_z}\right)^2 - \left(1 - \frac{J}{2\Delta B_z}\right)^2}}, \quad (8)$$

and thus offers J , n , and m as free parameters, noting that $J \ll \Delta B_z$. In condition (5), we replace the off-resonant Rabi frequency $\tilde{\Omega}$ with $\tilde{\Omega}_3 = \sqrt{(B_{y1,3}/2)^2 + (B_{z,3} - \omega_{\text{CNOT}})^2}$ and the driving time with $\tau_{\text{CNOT}} = |2\pi(2m+1)/\{B_{y1,1}[1 + J/(2\Delta B_z)]\}|$, and obtain the condition

$$\frac{(2m+1)\sqrt{\left(\frac{B_{y1,3}}{2}\right)^2 + (B_{z,3} - \omega_{\text{CNOT}})^2}}{B_{y1,1}\left(1 + \frac{J}{2\Delta B_z}\right)} = k, \quad (9)$$

for arbitrary $k \in \mathbb{Z}$. This leads to solutions for J depending on k , n , m and $\alpha = B_{y1,3}/B_{y1,1}$. To assure that $J \ll \Delta B_z$ holds and the assumptions made for the CNOT gate are valid, we only consider solutions with $|J| \leq (2\pi) 20$ MHz. We find that real-valued solutions only exist for $m = 0$ or $m = -1$ and we choose $m = 0$ from now onward.

In Fig. 4, our results for J , $B_{y1,1}$, and τ_{CNOT} are shown for various values of n and for $k = -50$, -100 , and -500 assuming $\alpha = 0.1$. The general trend in the plotted region is

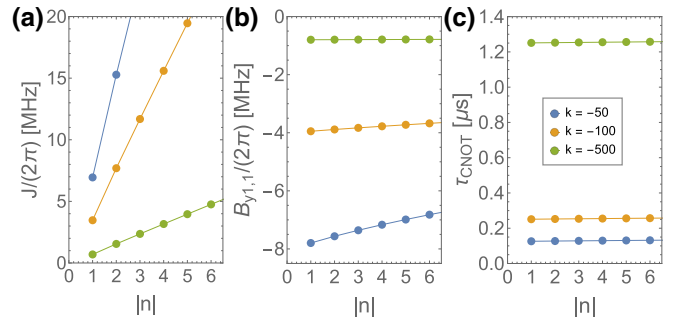


FIG. 4. Symmetric solutions for exchange coupling J , magnetic driving amplitude $B_{y1,1}$, and driving time τ_{CNOT} depending on n for $k = -50$, -100 , and -500 to simultaneously fulfill the CNOT and crosstalk synchronization conditions. Here, $B_{z,1} = (2\pi) 18.493$ GHz, $\Delta B_z = (2\pi) 0.2$ GHz, and $\alpha = 0.1$.

a linearly increasing positive value for J when n increases. Furthermore, when choosing higher k , more solutions emerge in the $(2\pi)20$ MHz regime, and hence we obtain a decreasing exchange interaction for an increasing absolute integer of k . On the other hand, when n or k increase, the absolute value of $B_{y1,1}$ decreases. For larger k , the slope and thus the impact of n is reduced. As a consequence of large driving amplitudes, due to $\tau_{\text{CNOT}} \propto |1/B_{y1,1}|$ longer gate times are required, which is why the choice of small n and k seems advantageous for our purpose. Nevertheless, the choice of k dominates the driving time for large integers k , which is why n is negligible for τ_{CNOT} . Moreover, better validity of the approximation using small J compared to the magnetic field gradient is possible at the cost of a longer gate time. Here it also turns out that a larger ratio between the induced and driving field does not increase J significantly. Although α determines the strength of crosstalk, it only slightly changes the conditioned values for synchronization due to high k values.

To provide an example, for the measured resonance frequencies $B_{z,1} = (2\pi) 18.493$ GHz, $B_{z,2} = (2\pi) 18.693$ GHz, $B_{z,3} = (2\pi) 18.893$ GHz, and $\alpha = 0.1$, we propose to set $k = 50$, $m = 0$, $n = 1$, and thus choose an exchange coupling $J = (2\pi) 7.0$ MHz and driving strength $B_{y1,1} = B_{y1,2} = (2\pi) 7.8$ MHz, which lead to a driving time of approximately 126 ns, to fulfill both CNOT and crosstalk synchronization conditions, and hence avoid crosstalk on nearest neighbors. The precision of these values is chosen sufficiently high such as to allow for an infidelity below 10^{-6} .

V. SIMULTANEOUSLY DRIVEN SINGLE-QUBIT GATES

In quantum algorithms, single-qubit gates are usually applied simultaneously due to the limited coherence times of qubits. Motivated by recent crosstalk measurements in Refs. [40] and [7,19], we further consider simultaneously driven Y gates on each of the two neighboring qubits 1 and 2, and investigate crosstalk effects. The second driving strength enters the Hamiltonian via the magnetic field in the y direction, which thus becomes $B_y(t) = B_{y0,i} + B_{y1,i} \cos(\omega_1 t + \theta_1) + B_{y2,i} \cos(\omega_2 t + \theta_2)$. Here we assume a symmetric crosstalk, i.e., $B_{y1,2} = \alpha B_{y1,1}$ and $B_{y2,1} = \alpha B_{y2,2}$. In the rotating frame defined by the transformation

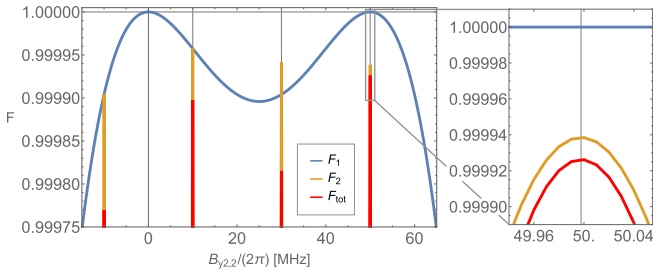


FIG. 5. Single-qubit fidelities F_1 , F_2 of qubits 1 (blue) and 2 (yellow), and two-qubit fidelity F_{tot} (red) for simultaneous Y gates on qubits 1 and 2 depending on $B_{y2,2}$, while $B_{y1,1}$ fulfills $(m_1 + 1/2)T_{q1} = 2\pi k/\Delta B_z$. F_1 shows a maximum which is close to a peak of F_2 at $B_{y2,2}$ values fulfilling $(2 + 1/2)T_{q2} = 2\pi k_2/\Delta B_z$, and thus F_{tot} becomes maximal.

$\tilde{R} = \exp[-i(\omega_1 \mathbf{S}_1 + \omega_2 \mathbf{S}_2)t]$, where ω_1 and ω_2 match the resonance frequencies of qubits 1 and 2, the RWA is invalid for close off-resonant Rabi oscillations with large driving amplitudes, $B_{y2,1}$ and $B_{y1,2}$. In this case, time-dependent terms remain and lead to the $2\pi/\Delta B_z$ periodic Hamiltonian,

$$\tilde{H} = \frac{1}{2} \begin{pmatrix} B_{y2,1} \sin(\Delta B_z t) \\ B_{y1,1} + B_{y2,1} \cos(\Delta B_z t) \\ 0 \end{pmatrix} \cdot \mathbf{S}_1 + \frac{1}{2} \begin{pmatrix} B_{y1,2} \sin(\Delta B_z t) \\ B_{y2,2} + B_{y1,2} \cos(\Delta B_z t) \\ 0 \end{pmatrix} \cdot \mathbf{S}_2. \quad (10)$$

An approximated description of the time evolution is given by the FME with up to second-order coefficients showing a periodicity with periods $T_{q\beta}$ given by

$$\left| \frac{16\pi \Delta B_z}{\sqrt{4B_{y\beta,\beta} B_{y\bar{\beta},\beta}^3 - 4B_{y\beta,\beta}^2 B_{y\bar{\beta},\beta}^2 - 16B_{y\beta,\beta}^2 \Delta B_z^2 - B_{y\bar{\beta},\beta}^4}} \right|, \quad (11)$$

where $\beta = 1, 2$ denotes the qubit number and $\bar{1} = 2$ and $\bar{2} = 1$. During the gate time τ_Y , both fields and their induced crosstalk fields on the neighbor are present. Choosing $B_{1,1}$ such that a π rotation of qubit 1 is fulfilled, i.e., $\tau_Y = (m_1 + 1/2)T_{q1}$ with integer $m_1 \in \mathbb{Z}$, the single-qubit fidelity of qubit 1 reaches a maximum when additionally $\tau_Y = 2\pi k/\Delta B_z$ with integer $k \in \mathbb{Z}$ is fulfilled. Since τ_Y grows linearly but fidelities increase with k , we choose $k = 20$ which, for $\Delta B_z = (2\pi) 0.2$ GHz, leads to a gate time of 100 ns, and set $m_1 = 0$ from now on. Varying $B_{y2,1}$ shows a second fidelity maximum besides the trivial one for qubit 1 as in Fig. 5 (blue), which occurs if $B_{y1,1}$ becomes maximal within both conditions for τ_Y . Advantageously, for $\alpha = 0.4$, this maximum appears close to $B_{y2,2}$ fulfilling $\tau_Y = (m_2 + 1/2)T_{q2}$ with $m_2 = 2$, which is given at the maxima of the qubit 2 fidelity (yellow). Also, the two-qubit fidelity in Fig. 5 (red) indeed becomes maximum at this point. Due to the assumption of symmetric crosstalk, the same behavior is obtained when swapping qubits 1 and 2. For arbitrary α , a combination of m_1 , m_2 , and k can be found to bring the maxima of both single-qubit fidelities close together and thus nearly fulfill all of the above con-

ditions for the magnetic fields and driving time. For $B_z = (2\pi) 18.493$ GHz, $\Delta B_z = (2\pi) 0.2$ GHz, $\alpha = 0.4$, $m_1 = 0$, and $k = 20$, we find $1 - F_1 = 3.54 \times 10^{-12}$ and $1 - F_2 = 6.14 \times 10^{-5}$ for the single-qubit infidelities of qubits 1 and 2, and $1 - F = 7.37 \times 10^{-5}$ for the two-qubit infidelity where $B_{y1,1} = (2\pi) 10$ MHz and $B_{y2,2} = (2\pi) 50$ MHz. Subsequent single-qubit z rotations or continuing driving one of the qubits does not improve the fidelity. Hence, we obtain an unavoidable crosstalk effect for simultaneously driven spin qubits. However, to further suppress this effect in linear spin qubit chains, we propose a three-step operation to perform single-qubit operations simultaneously. In each step, only every third qubit is acted on at the same time, such that after three steps, each qubit has been active once. For each step, the driving strength can be chosen such that one neighbor qubit is synchronized by the condition (5) and the other neighbor is nearly synchronized, as discussed in Sec. IV A. In this way, crosstalk errors become minimal and the time for simultaneously performing single-qubit rotations scales with a fixed factor of 3.

VI. CHARGE NOISE ANALYSIS

Fluctuations of electric field amplitudes in silicon spin qubit devices represent a great challenge for coherence times and unitarity of control sequences [41]. Charge noise couples to spins via spin-orbit coupling, magnetic field gradients, and exchange coupling, which determine detuning, and thus Rabi frequencies in a CNOT gate. Since the impact of charge noise via EDSR is rather small compared to the exchange coupling [6], usually fluctuations δJ of J are considered. This dominant charge noise contribution does not appear for single-qubit rotations and only affects the CNOT synchronization in Eq. (4), and thus the CNOT gate fidelity, which was already discussed in Ref. [16]. The crosstalk synchronization condition (5) for a neighboring qubit depends on its off-resonant Rabi frequency and driving time, and hence driving field and detuning. Since the neighboring qubit does not interact with other qubits, both driving and detuning are independent of J fluctuations, and so the synchronization to avoid crosstalk is, to a large extent, unaffected by charge noise.

Here, we consider fluctuations of driving amplitudes due to charge noise during EDSR, where the impact on crosstalk synchronization is no longer negligible. Assuming a precise driving time and nonfluctuating driving frequencies, we consider the diagonal and off-diagonal time evolution terms $U_{\text{diag}} = \cos(\tilde{\Omega}_{\text{NN}t}/2) \mp i(\delta\omega_z/\tilde{\Omega}_{\text{NN}}) \sin(\tilde{\Omega}_{\text{NN}t}/2)$ and $U_{\text{off-diag}} = \pm(\Omega_{\text{NN}}/\tilde{\Omega}_{\text{NN}}) \sin(\tilde{\Omega}_{\text{NN}t}/2)$ of the neighboring qubit describing Rabi oscillation, and calculate the first-order correction in Appendix B, which, for the synchronization condition (5), holds,

$$U_{\text{diag}} = 1 + i \left| \frac{\pi(2m+1)\alpha}{4\delta\omega_z} \left(1 - \frac{(2m+1)^2\alpha^2}{4k^2} \right) \right| \delta B, \quad (12)$$

$$U_{\text{off-diag}} = \left| \frac{(2m+1)^3\pi\alpha^2}{16k^2\delta\omega_z} \sqrt{\frac{4k^2}{(2m+1)^2\alpha^2} - 1} \right| \delta B, \quad (13)$$

where δB denotes the fluctuation in the effective magnetic field caused by charge noise.

Accordingly, Rabi oscillations are sensitive to first-order fluctuations of B_{NN} , which arise, e.g., through charge

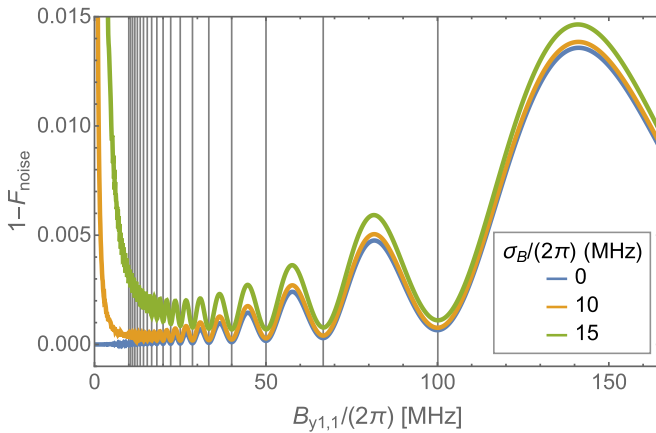


FIG. 6. Total memory infidelity in the presence of crosstalk with first-order noise correction in the Hamiltonian of neighboring qubit 2 for the Y gate as a function of the driving field strength $B_{y1,1}$ for three standard deviation values σ_B of the noise in the effective magnetic field, where $\delta\omega_z = (2\pi)0.2$ GHz and $\alpha = 0.4$. Vertical lines represent driving fields fulfilling the condition (5).

fluctuations in the EDSR driving field. Nevertheless, applying the synchronization condition yields terms with $(2m+1)^2/k$ and $(2m+1)^3/k^2$ dependence and thus makes it possible to reduce first-order noise due to short driving times and high k values. The major effect of noise is obtained for the imaginary diagonal part and can be reduced by using short driving times and larger detuning $\delta\omega_z$. Furthermore, numerical evaluation of our system with $\delta\omega_z = (2\pi)0.2$ GHz and $\alpha = 0.4$ shows that zeros of the first-order noise contribution to the off-diagonal terms are close to the synchronization condition (5) for the Y gate. Since diagonal relative noise contributions are smaller than those for the off-diagonal terms, noise becomes minimal at these points. In Fig. 6, the total infidelity of first-order corrections in the Hamiltonian ($B_{y1,2} \rightarrow B_{y1,2} + \delta B$) for a zero-mean Gaussian error with standard deviations σ_B of 0 MHz, $(2\pi)10$ MHz, and $(2\pi)15$ MHz is shown, where one indeed finds noise to be minimal close to magnetic driving fields $B_{y1,1}$ fulfilling the condition (5). Similar behavior is obtained for the CNOT gate implementation. Consequently, we find the crosstalk synchronization to be robust under charge noise.

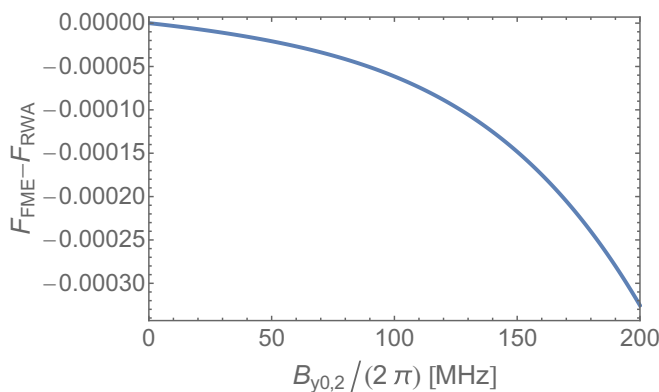


FIG. 7. Impact of the first Floquet-Magnus correction on the neighbor qubit fidelity for increasing $B_{y0,2}$ when performing a Y gate.

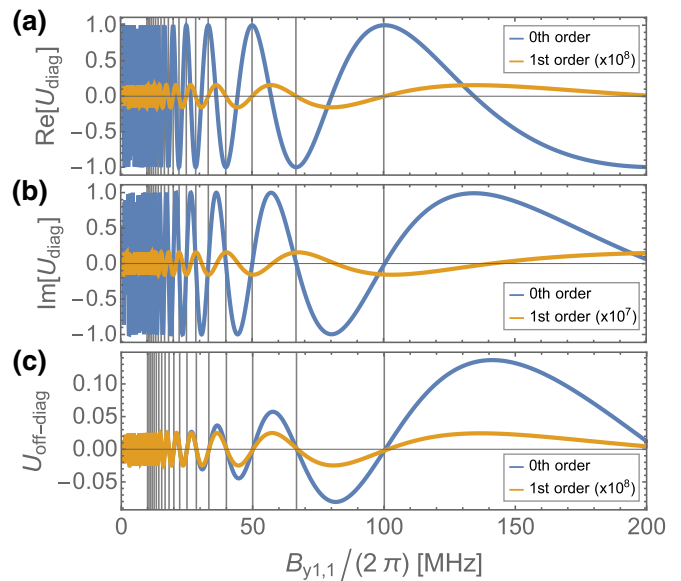


FIG. 8. First-order noise correction to (a) real and (b) imaginary diagonal and (c) off-diagonal Rabi terms of the neighboring qubit for the Y gate with $\delta\omega_z = \Delta B_z = (2\pi)0.2$ GHz and $\alpha = 0.4$, where vertical lines mark $B_{y1,1}$ values matching the synchronization condition.

Advantageous design enables qubits to be only higher-order sensitive to charge noise by operating at the sweet spot [10–12], which mostly reduces the above-discussed effects. The main reduction in fidelity for the CNOT gate operation caused by δJ can be further decreased by applying advanced pulse shaping [42] or dynamical decoupling sequences [37].

VII. CONCLUSIONS

In this paper, we have analyzed the effect of crosstalk of single-qubit and two-qubit gates on spin qubits and its impact on the fidelity starting from a simple Heisenberg model. We clarified the validity of the RWA in our system and are able to determine a fidelity dependence for magnetic field gradients in the y direction which can invalidate the RWA. Here we explicitly considered rotations around the y axis, which together with frame rotations around the z axis enable arbitrary single-qubit operations. Since dc driven two-qubit gates as the CPHASE and $\sqrt{\text{SWAP}}$ only require a square pulse, their crosstalk effects can mostly be avoided by virtual gates. Here we consider a CNOT as a two-qubit gate, which is operated in the $J \ll \Delta B_z$ regime and driven with an ac pulse. We showed that the underlying effect for crosstalk is the same for single-qubit and ac driven two-qubit gates, namely, a residual driving field at neighboring qubits leading to off-resonant Rabi oscillations.

Moreover, we considered techniques to minimize crosstalk besides existing dynamical decoupling schemes and suggested a virtual gate realization for driving fields. We also demonstrated how software implementations of subsequent z rotations can significantly increase the fidelity. Then we proposed a synchronization of Rabi frequencies to avoid crosstalk and gave synchronization conditions for the single-qubit Y gate and the two-qubit CNOT gate. This idea is in general applicable to any device suffering from crosstalk via

off-resonant Rabi oscillations and only requires the knowledge of the off-resonant Rabi frequencies and precise control of driving strength and time. Furthermore, the synchronization protocol can also be adapted to partial π rotations and thus is compatible with spin echo pulsing leading to even higher fidelities in experimental setups. We also showed that double synchronization with two neighboring qubits is possible, in principle, under some additional constraints and requires precise hardware fabrication and knowledge to exactly determine the capacitive coupling between driving gates. For multiple neighbors of an operating qubit with arbitrary couplings as in qubit arrays, an exact synchronization of one qubit, e.g., the most affected one, is possible and approximate synchronizations of the other neighbors can be found. For a detailed solution for a given number of neighboring qubits, further work is required and goes beyond the scope of this paper. We gave realistic exchange interactions and driving strengths to perform mostly crosstalk-free Y and CNOT gates and thus suggested a robust high-fidelity gate implementation for scaled-up systems containing multiple quantum dot spin qubits. For simultaneously driven single-qubit rotations, we found fidelity maximizing conditions for driving time and strengths and suggested a three-step application of simultaneous gates to reduce and control crosstalk, and therefore speed up and improve quantum algorithms on spin qubit devices.

ACKNOWLEDGMENTS

This work has been supported by QLSI with funding from the European Union's Horizon 2020 research and innovation programme under Grant Agreement No. 951852 and by the Deutsche Forschungsgemeinschaft (DFG, German Research Foundation) Grant No. SFB 1432, Project ID No. 425217212.

APPENDIX A: FLOQUET-MAGNUS EXPANSION

To investigate the validity of the RWA, we plot the impact of the first-order Floquet-Magnus correction [28–31] on the fidelity depending on $B_{y0,2}$ of the neighbor qubit 2 when performing a Y gate on qubit 1 in Fig. 7, with $B_{z,1} = (2\pi) 18.483$ GHz, $\Delta B_z = (2\pi) 0.2$ GHz, $B_{y1,1} = (2\pi) 200$ MHz, and $B_{y1,2} = 0.4 B_{y1,1}$. Indeed, RWA shows to be a valid approximation in our case and we can determine the fidelity impairment for a given value of $B_{y0,2}$.

APPENDIX B: CHARGE NOISE ANALYSIS

For a charge noise analysis assuming fluctuations in the EDSR driving fields $B_{y1,1}$ and $B_{y1,2}$, matrix elements of the neighbor qubit Hamiltonian causing Rabi oscillations are considered. First-order corrected diagonal and off-diagonal elements are given by

$$U_{\text{diag}} = \cos\left(\frac{\tilde{\Omega}_{\text{NN}} t}{2}\right) \mp \frac{i\delta\omega_z}{\tilde{\Omega}_{\text{NN}}} \sin\left(\frac{\tilde{\Omega}_{\text{NN}} t}{2}\right) + \left| \frac{\Omega_{\text{NN}}}{2\tilde{\Omega}_{\text{NN}}} \left(-\frac{t}{2} \mp \frac{i\delta\omega_z}{\tilde{\Omega}_{\text{NN}}^2}\right) \sin\left(\frac{\tilde{\Omega}_{\text{NN}} t}{2}\right) \mp \frac{i\delta\omega_z \Omega_{\text{NN}} t}{4\tilde{\Omega}_{\text{NN}}^2} \cos\left(\frac{\tilde{\Omega}_{\text{NN}} t}{2}\right) \right| \delta B, \quad (\text{B1})$$

$$U_{\text{off-diag}} = \pm \frac{\Omega_{\text{NN}}}{\tilde{\Omega}_{\text{NN}}} \sin\left(\frac{\tilde{\Omega}_{\text{NN}} t}{2}\right) + \left| \pm \frac{\delta\omega_z^2}{2\tilde{\Omega}_{\text{NN}}^3} \sin\left(\frac{\tilde{\Omega}_{\text{NN}} t}{2}\right) \mp \frac{\Omega_{\text{NN}}^2 t}{4\tilde{\Omega}_{\text{NN}}^2} \cos\left(\frac{\tilde{\Omega}_{\text{NN}} t}{2}\right) \right| \delta B. \quad (\text{B2})$$

First-order corrections of the diagonal and off-diagonal terms are shown in Fig. 8 for the Y gate, where for clarity reasons noise amplitudes are multiplied with factors 10^8 and 10^7 , respectively. Ideally, the absolute value of the real diagonal part should be 1, while the imaginary diagonal and the off-diagonal parts should be zero, which is fulfilled for the zeroth-order terms at synchronization. Apparently, the first-order real diagonal part is canceled and the off-diagonal part is almost zero when $B_{y1,1}$ fulfills the crosstalk synchronization condition. The remaining imaginary diagonal noise contribution relative to zeroth order is approximately one

magnitude smaller than the off-resonant contribution, which is why the overall noise contribution is nearly minimal at synchronization, as shown in the infidelity plot of Fig. 6, where for first-order zero-mean Gaussian noise with σ_B of 0 MHz, $(2\pi) 10$ MHz, and $(2\pi) 15$ MHz, the total infidelity is plotted. Similar behavior is obtained for the CNOT gate where the first-order noise amplitude relative to the zeroth-order amplitude of the imaginary part is even smaller compared to the off-diagonal term. For the values used and proposed in this paper, crosstalk synchronization is hardly sensitive to first-order noise via EDSR field fluctuations, and thus shows to be robust.

- [1] D. Loss and D. P. DiVincenzo, Quantum computation with quantum dots, *Phys. Rev. A* **57**, 120 (1998).
- [2] F. A. Zwanenburg, A. S. Dzurak, A. Morello, M. Y. Simmons, L. C. L. Hollenberg, G. Klimeck, S. Rogge, S. N. Coppersmith, and M. A. Eriksson, Silicon quantum electronics, *Rev. Mod. Phys.* **85**, 961 (2013).
- [3] M. Veldhorst, J. C. C. Hwang, C. H. Yang, A. W. Leenstra, B. de Ronde, J. P. Dehollain, J. T. Muhonen, F. E. Hudson, K. M. Itoh, A. Morello *et al.*, An addressable quantum dot qubit with fault-tolerant control-fidelity, *Nat. Nanotechnol.* **9**, 981 (2014).

- [4] T. D. Ladd and M. S. Carroll, Silicon qubits, in *Encyclopedia of Modern Optics*, 2nd ed., edited by B. D. Guenther and D. G. Steel (Elsevier, Oxford, 2018), Vol. 1, pp. 467–477.
- [5] G. Burkard, D. Loss, and D. P. DiVincenzo, Coupled quantum dots as quantum gates, *Phys. Rev. B* **59**, 2070 (1999).
- [6] J. Yoneda, K. Takeda, T. Otsuka, T. Nakajima, M. R. Delbecq, G. Allison, T. Honda, T. Kodera, S. Oda, Y. Hoshi *et al.*, A quantum-dot spin qubit with coherence limited by charge noise and fidelity higher than 99.9%, *Nat. Nanotechnol.* **13**, 102 (2017).

- [7] T. F. Watson, S. G. J. Philips, E. Kawakami, D. R. Ward, P. Scarlino, M. Veldhorst, D. E. Savage, M. G. Lagally, M. Friesen, S. N. Coppersmith *et al.*, A programmable two-qubit quantum processor in silicon, *Nature (London)* **555**, 633 (2018).
- [8] D. M. Zajac, A. J. Sigillito, M. Russ, F. Borjans, J. M. Taylor, G. Burkard, and J. R. Petta, Resonantly driven CNOT gate for electron spins, *Science* **359**, 439 (2017).
- [9] R. Brunner, Y.-S. Shin, T. Obata, M. Pioro-Ladrière, T. Kubo, K. Yoshida, T. Taniyama, Y. Tokura, and S. Tarucha, Two-Qubit Gate of Combined Single-Spin Rotation and Interdot Spin Exchange in a Double Quantum Dot, *Phys. Rev. Lett.* **107**, 146801 (2011).
- [10] F. Martins, F. K. Malinowski, P. D. Nissen, E. Barnes, S. Fallahi, G. C. Gardner, M. J. Manfra, C. M. Marcus, and F. Kuemmeth, Noise Suppression Using Symmetric Exchange Gates in Spin Qubits, *Phys. Rev. Lett.* **116**, 116801 (2016).
- [11] M. D. Reed, B. M. Maune, R. W. Andrews, M. G. Borselli, K. Eng, M. P. Jura, A. A. Kiselev, T. D. Ladd, S. T. Merkel, I. Milosavljevic, E. J. Pritchett, M. T. Rakher, R. S. Ross, A. E. Schmitz, A. Smith, J. A. Wright, M. F. Gyure, and A. T. Hunter, Reduced Sensitivity to Charge Noise in Semiconductor Spin Qubits via Symmetric Operation, *Phys. Rev. Lett.* **116**, 110402 (2016).
- [12] B. Bertrand, H. Flentje, S. Takada, M. Yamamoto, S. Tarucha, A. Ludwig, A. D. Wieck, C. Bäuerle, and T. Meunier, Quantum Manipulation of Two-Electron Spin States in Isolated Double Quantum Dots, *Phys. Rev. Lett.* **115**, 096801 (2015).
- [13] J. M. Nichol, L. A. Orona, S. P. Harvey, S. Fallahi, G. C. Gardner, M. J. Manfra, and A. Yacoby, High-fidelity entangling gate for double-quantum-dot spin qubits, *NPJ Quantum Inf.* **3**, 3 (2017).
- [14] J. Yoneda, T. Otsuka, T. Takakura, M. Pioro-Ladrière, R. Brunner, H. Lu, T. Nakajima, T. Obata, A. Noiri, C. J. Palmstrøm *et al.*, Robust micromagnet design for fast electrical manipulations of single spins in quantum dots, *Appl. Phys. Express* **8**, 084401 (2015).
- [15] E. Kawakami, P. Scarlino, D. R. Ward, F. R. Braakman, D. E. Savage, M. G. Lagally, M. Friesen, S. N. Coppersmith, M. A. Eriksson, and L. M. K. Vandersypen, Electrical control of a long-lived spin qubit in a Si/SiGe quantum dot, *Nat. Nanotechnol.* **9**, 666 (2014).
- [16] M. Russ, D. M. Zajac, A. J. Sigillito, F. Borjans, J. M. Taylor, J. R. Petta, and G. Burkard, High-fidelity quantum gates in Si/SiGe double quantum dots, *Phys. Rev. B* **97**, 085421 (2018).
- [17] D. M. Zajac, T. M. Hazard, X. Mi, E. Nielsen, and J. R. Petta, Scalable Gate Architecture for a One-Dimensional Array of Semiconductor Spin Qubits, *Phys. Rev. Appl.* **6**, 054013 (2016).
- [18] R. Ferdous, K. W. Chan, M. Veldhorst, J. C. C. Hwang, C. H. Yang, H. Sahasrabudhe, G. Klimeck, A. Morello, A. S. Dzurak, and R. Rahman, Interface-induced spin-orbit interaction in silicon quantum dots and prospects for scalability, *Phys. Rev. B* **97**, 241401 (2018).
- [19] X. Xue, T. F. Watson, J. Helsen, D. R. Ward, D. E. Savage, M. G. Lagally, S. N. Coppersmith, M. A. Eriksson, S. Wehner, and L. M. K. Vandersypen, Benchmarking Gate Fidelities in a Si/SiGe Two-Qubit Device, *Phys. Rev. X* **9**, 021011 (2019).
- [20] F. H. L. Koppens, C. Buizert, K. J. Tielrooij, I. T. Vink, K. C. Nowack, T. Meunier, L. P. Kouwenhoven, and L. M. K. Vandersypen, Driven coherent oscillations of a single electron spin in a quantum dot, *Nature (London)* **442**, 766 (2006).
- [21] R. Li, L. Petit, D. P. Franke, J. P. Dehollain, J. Helsen, M. Steudtner, N. K. Thomas, Z. R. Yoscovits, K. J. Singh, S. Wehner *et al.*, A crossbar network for silicon quantum dot qubits, *Sci. Adv.* **4**, eaar3960 (2018).
- [22] V. N. Golovach, M. Borhani, and D. Loss, Electric-dipole-induced spin resonance in quantum dots, *Phys. Rev. B* **74**, 165319 (2006).
- [23] Y. Tokura, W. G. van der Wiel, T. Obata, and S. Tarucha, Coherent Single Electron Spin Control in a Slanting Zeeman Field, *Phys. Rev. Lett.* **96**, 047202 (2006).
- [24] L. H. Pedersen, N. M. Møller, and K. Mølmer, Fidelity of quantum operations, *Phys. Lett. A* **367**, 47 (2007).
- [25] J. Cayao, M. Benito, and G. Burkard, Programable two-qubit gates in capacitively coupled flopping-mode spin qubits, *Phys. Rev. B* **101**, 195438 (2020).
- [26] S. F. Neyens, E. R. MacQuarrie, J. P. Dodson, J. Corrigan, N. Holman, B. Thorgrimsson, M. Palma, T. McJunkin, L. F. Edge, M. Friesen, S. N. Coppersmith, and M. A. Eriksson, Measurements of Capacitive Coupling Within a Quadruple-Quantum-Dot Array, *Phys. Rev. Appl.* **12**, 064049 (2019).
- [27] K. C. Nowack, F. H. L. Koppens, Y. V. Nazarov, and L. M. K. Vandersypen, Coherent control of a single electron spin with electric fields, *Science* **318**, 1430 (2007).
- [28] M. Bukov, L. D'Alessio, and A. Polkovnikov, Universal high-frequency behavior of periodically driven systems: From dynamical stabilization to Floquet engineering, *Adv. Phys.* **64**, 139 (2015).
- [29] S. Blanes, F. Casas, J. Oteo, and J. Ros, The magnus expansion and some of its applications, *Phys. Rep.* **470**, 151 (2009).
- [30] D. J. Moore, Floquet theory and the non-adiabatic Berry phase, *J. Phys. A* **23**, L665 (1990).
- [31] A. Mostafazadeh, Quantum adiabatic approximation and the geometric phase, *Phys. Rev. A* **55**, 1653 (1997).
- [32] T. Obata, M. Pioro-Ladrière, Y. Tokura, Y.-S. Shin, T. Kubo, K. Yoshida, T. Taniyama, and S. Tarucha, Coherent manipulation of individual electron spin in a double quantum dot integrated with a micromagnet, *Phys. Rev. B* **81**, 085317 (2010).
- [33] A. R. Mills, D. M. Zajac, M. J. Gullans, F. J. Schupp, T. M. Hazard, and J. R. Petta, Shuttling a single charge across a one-dimensional array of silicon quantum dots, *Nat. Commun.* **10**, 1063 (2019).
- [34] T. Hensgens, T. Fujita, L. Janssen, X. Li, C. J. Van Diepen, C. Reichl, W. Wegscheider, S. Das Sarma, and L. M. K. Vandersypen, Quantum simulation of a Fermi-Hubbard model using a semiconductor quantum dot array, *Nature (London)* **548**, 70 (2017).
- [35] T.-K. Hsiao, C. J. van Diepen, U. Mukhopadhyay, C. Reichl, W. Wegscheider, and L. M. K. Vandersypen, Efficient Orthogonal Control of Tunnel Couplings in a Quantum Dot Array, *Phys. Rev. Appl.* **13**, 054018 (2020).
- [36] D. Buterakos, R. E. Throckmorton, and S. Das Sarma, Crosstalk error correction through dynamical decoupling of single-qubit gates in capacitively coupled singlet-triplet semiconductor spin qubits, *Phys. Rev. B* **97**, 045431 (2018).
- [37] S. Blanvillain, J. I. Colless, D. J. Reilly, H. Lu, and A. C. Gossard, Suppressing on-chip electromagnetic crosstalk

- for spin qubit devices, *J. Appl. Phys.* **112**, 064315 (2012).
- [38] R. Hanson, L. P. Kouwenhoven, J. R. Petta, S. Tarucha, and L. M. K. Vandersypen, Spins in few-electron quantum dots, *Rev. Mod. Phys.* **79**, 1217 (2007).
- [39] C. Volk, A. M. J. Zwerver, U. Mukhopadhyay, P. T. Eendebak, C. J. van Diepen, J. P. Dehollain, T. Hensgens, T. Fujita, C. Reichl, W. Wegscheider *et al.*, Loading a quantum-dot based qubyte register, *NPJ Quantum Inf.* **5**, 29 (2019).
- [40] F. Fedele, A. Chatterjee, and F. Kuemmeth, Simultaneous operation of singlet-triplet qubits, in *2019 Silicon Nanoelectronics Workshop (SNW)* (2019) pp. 1–2.
- [41] E. Paladino, Y. M. Galperin, G. Falci, and B. L. Altshuler, $1/f$ noise: Implications for solid-state quantum information, *Rev. Mod. Phys.* **86**, 361 (2014).
- [42] L. M. K. Vandersypen and I. L. Chuang, NMR techniques for quantum control and computation, *Rev. Mod. Phys.* **76**, 1037 (2005).